

Tunneling through an Anderson impurity between superconductors

YshaiAvishai¹, Anatoly Golub¹ and Andrei D. Zaikin^{2,3}¹ Department of Physics, Ben-Gurion University of the Negev, Beer-Sheva, Israel² Forschungszentrum Karlsruhe, Institut für Nanotechnologie, 76021 Karlsruhe, Germany³ I.E.Tamm Department of Theoretical Physics, P. N. Lebedev Physics Institute, 117924 Moscow, Russia
(April 14, 2024)

We consider an Anderson impurity (A) weakly connected to a superconducting electrode (S) on one side and a superconducting or a normal metal electrode (N) on the other side. A general path integral formalism is developed and the response of SAN and SAS junctions to a constant voltage bias V is elucidated, using a combination of the Keldysh technique (to handle non-equilibrium effects) and a dynamical mean field approximation (to handle repulsive Hubbard interactions). An interesting physics is exposed at sub-gap voltages ($eV < \Delta$ for SAN and $eV < 2\Delta$ for SAS). For an SAN junction, Andreev reflection is strongly affected by Coulomb interaction. For superconductors with p-wave symmetry the junction conductance exhibits a remarkable peak at $eV < \Delta$, while for superconductors with s-wave symmetric pair potential the peak is shifted towards the gap edge $eV = \Delta$ and strongly suppressed if the Hubbard repulsive interaction increases. Electron transport in SAS junctions is determined by an interplay between multiple Andreev reflection (MAR) and Coulomb effects. For s-wave superconductors the usual peaks in the conductance that originate from MAR are shifted by interaction to larger values of V . They are also suppressed as the Hubbard interaction strength grows. For p-wave superconductors the sub-gap current is much larger and the $I-V$ characteristics reveal a new feature, namely, a peak in the current resulting from a mid-gap bound state in the junction.

I. INTRODUCTION

The dynamical behavior of Josephson junction strongly depends, among other factors, on its transparency. If the insulating barrier is not too high then the concept of nonlinear tunneling becomes relevant. In this case the characteristic dynamical conductance dI/dV at applied voltages V less than the superconducting gap shows a sub-gap structure. An explanation of this behavior was given some time ago [1,2], based on the mechanisms of multiple Andreev reflections (MAR). Recently, the sub-gap current was calculated for the case of electron tunneling through a junction with resonant impurity [3]. Rapid progress in the technology of superconducting junctions makes it possible to fabricate junctions composed of quantum dots weakly coupled to superconducting or normal electrodes. The basic physics of such a device can be elucidated once it is modeled as an Anderson impurity center. In this case the Coulomb interaction is expected to strongly affect the tunneling current in general and the sub-gap current in particular. Since the sub-gap current is originated from multiple Andreev reflections, its physics has a close similarity to that of the Josephson current. In this context, it is established [4] that the tunneling through a quantum dot is suppressed if the effective Kondo temperature $T_K = U \exp[-j_0/2]$ is small as compared to the superconducting gap Δ . Hereafter, U is the Hubbard

repulsion strength, ϵ_0 is the orbital energy of the dot electron and Γ is the width of this energy state. Strong interaction-induced suppression of the current through superconducting quantum dots was also observed experimentally [5].

Quite recently detailed measurements of the $I-V$ curves in atomic-size metallic contacts were performed [6]. An explanation of the observed $I-V$ curves were given [7] in terms of the atomic valence orbitals which represent different conducting channels. The Coulomb interaction was considered there to be screened as in bulk metals. However, for quantum dots and break junctions the screening is virtually ineffective and an unscreened Hubbard-type repulsive interaction emerges. In this case the Kondo temperature T_K becomes a relevant parameter, separating levels with $T_K > \Delta$ (which are responsible for high, nearly resonant conductance) from levels with $T_K < \Delta$, in which the conductance is strongly influenced by interaction.

One of the main goals of the present paper is to develop a detailed theoretical analysis of an interplay between the phenomena of multiple Andreev reflections and Coulomb interaction in superconducting quantum dots. Even though both MAR and Coulomb effects have been intensively studied in the literature over past decades, an interplay between them (to the best of our knowledge) was not elucidated until now. In this paper we will demonstrate that these two phenomena, being combined in superconducting quantum dots, lead to novel physical effects and (depending on parameters) may dramatically influence the sub-gap conductance pattern of the system. In short, Coulomb suppression of MAR turns out to be much more pronounced than, say, that of

single electron tunneling. This is because during MAR cycles at relatively low voltages the charge is transferred by large quanta, much larger than the electron charge e .

Another important issue in the study of SAS and SAN junctions is the parity of the order parameter of the superconducting electrodes. For example, the order parameter of the recently discovered [8] superconducting material Sr_2RuO_4 is believed to have a p-wave symmetry [9]. If a superconductor of this type is properly oriented with respect to the tunneling direction the principal contribution to the Josephson current comes from a bound state [10,11] formed at the contact point. This bound state arises since the pair potential has an opposite sign for injected and reflected quasiparticles and is expected to play an important role in the formation of sub-gap currents.

In the present work we expose the physics of SAS and SAN junctions subject to a finite potential bias. In particular, we calculate the tunneling current and the dynamical conductance for junctions consisting of s- and p-wave superconductors. The main steps required for treating the pertinent many-body problem can be summarized as follows: 1) Taking the Fermi energy of the unbiased lead as an energy reference, the site energy ϵ_0 of the Anderson impurity is chosen such that $\epsilon_0 < 0$ while $U + \epsilon_0 > 0$. These inequalities assure that assuming the quantum dot to be at most singly occupied should be an excellent approximation. 2) To handle the strong interaction appearing in the Hubbard term, a mean field approximation [12,13] is adopted. 3) The formalism should take into account the nonequilibrium nature of the physical system. For this purpose, the standard approach is to start from the expression for the kernel of the evolution operator or the generating functional, which is the analog of the partition function in the equilibrium case, evaluated, however, on a Keldysh contour [14] (see review article in Ref. [15]). At the end of this procedure one is able to calculate the SAN Andreev conductance analytically, and to get expressions for the non-linear response of SAS junctions which are amenable for numerical evaluation.

The technical procedure by which we manage to advance the calculations is detailed below in section 2, where we derive an effective action for SAS and SAN junctions. In section 3 we discuss the dynamical mean field approximation adopted in the present work in order to treat interaction effects. Concrete results pertaining to sub-gap current in SAS junctions and differential conductance in SAN junctions are presented and discussed in section 4. The paper is then concluded and summarized in section 5. Some technical details of the calculation are given in Appendix.

II. GENERAL ANALYSIS

A. The Model

Consider a system consisting of two superconducting wide strips on the left ($x < 0$; $-1 < y < 1$) and on the right ($x > 0$; $-1 < y < 1$) weakly connected by a quantum dot through which an electron tunneling takes place. This system can be described by the Hamiltonian

$$H = H_L + H_R + H_{\text{dot}} + H_t; \quad (1)$$

The Hamiltonians of the left and right superconducting electrodes have the standard BCS form

$$H_j = \sum_{\mathbf{r}} \text{dr} \left[\sum_{\mathbf{j}} \psi_{\mathbf{j}}^{\dagger}(\mathbf{r}) (\epsilon_{\mathbf{j}} - \mu) \psi_{\mathbf{j}}(\mathbf{r}) + \sum_{\mathbf{j}} \psi_{\mathbf{j}}^{\dagger}(\mathbf{r}) \psi_{\mathbf{j}\#}^{\dagger}(\mathbf{r}) \Delta_{\mathbf{j}} + \text{h.c.} \right]; \quad (2)$$

Here $\psi_{\mathbf{j}}^{\dagger}(\mathbf{r})$ ($\psi_{\mathbf{j}}(\mathbf{r})$) are the electron creation (annihilation) operators, $\Delta_{\mathbf{j}}$ is the BCS coupling constant, $\epsilon_{\mathbf{j}} = \epsilon_0 + \mathbf{r}^2/2m$ and $\mathbf{j} = L, R$. Here and below we set the Planck's constant $\hbar = 1$. Whenever appropriate, the spin, space and time dependence of all the field operators will not be explicitly displayed.

The quantum dot is treated as an Anderson impurity center located at $x = y = 0$. It is described by the Hamiltonian

$$H_{\text{dot}} = \epsilon_0 \sum_{\sigma} c_{\sigma}^{\dagger} c_{\sigma} + U \sum_{\sigma} c_{\sigma}^{\dagger} c_{\sigma} c_{\sigma\#}^{\dagger} c_{\sigma\#}; \quad (3)$$

where c_{σ}^{\dagger} and c_{σ} are the electron operators in the dot. The impurity site energy ϵ_0 (counted from the Fermi energy) is assumed to be far below the Fermi level $\epsilon_0 < 0$. The presence of a strong Coulomb repulsion $U > 0$ between electrons in the same orbital guarantees that the dot is at most singly occupied.

Electron tunneling through the dot is accounted for by means of the term,

$$H_t = \sum_{\mathbf{j}=L,R} \sum_{\mathbf{j}'} T_{\mathbf{j}\mathbf{j}'} \sum_{\mathbf{r}} \psi_{\mathbf{j}}^{\dagger}(\mathbf{r}) c_{\mathbf{r}} + \text{h.c.}; \quad (4)$$

where $T_{L(R)}$ are the effective transfer amplitudes between the left (right) electrode and the dot.

In what follows we will always assume that, if a bias voltage V is applied to the system from, say, right to left, the entire voltage drop occurs across the dot. Hence, the quasiparticle distribution functions in the leads are the Fermi ones, with the chemical potentials of the electrodes shifted with respect to each other by eV .

B. Evolution Operator

Complete information about the quantum dynamics of the system is contained within the evolution operator defined on the Keldysh contour [14] K (which consists of

forward and backward oriented time branches). The kernel J of this evolution operator can be expressed in terms of a path integral,

$$J = \int \mathcal{D}c \mathcal{D}c^\dagger \mathcal{D}\psi \mathcal{D}\psi^\dagger \exp(iS); \quad (5)$$

over the fermion fields corresponding to the operators $\psi_L^\dagger, \psi_L, \psi_R^\dagger, \psi_R$ and c (here the field c corresponds to $(\psi_L^\dagger; \psi_L^\dagger; \psi_R^\dagger; \psi_R^\dagger)$ and similarly for other fields), $S = \int_K L dt$ is the action and L is the Lagrangian pertaining to the Hamiltonian (1). The external fields (e.g. electromagnetic fields) can be treated as the source terms for the action, though, the fluctuating parts of these fields should be integrated as well.

Usually it is convenient to perform an operator rotation $c \rightarrow \hat{Q}c$ and $\psi \rightarrow \hat{Q}\psi$ in Keldysh space:

$$c = \hat{Q}^{-1} c; \quad c^\dagger = \hat{Q} c^\dagger; \quad \psi = \hat{Q}^{-1} \psi; \quad \psi^\dagger = \hat{Q} \psi^\dagger; \quad (6)$$

Here \hat{Q} is one of the Pauli matrices $\sigma_x, \sigma_y, \sigma_z$ operating in the Keldysh space and

$$\hat{Q} = \frac{1}{2} \begin{pmatrix} 1 & 1 \\ 1 & 1 \end{pmatrix} \quad (7)$$

is the Keldysh matrix. The Grassman variables $c, c^\dagger, \psi, \psi^\dagger$ are now defined solely on the forward time branch.

The transformation of the Green functions follows directly from (6). One starts from the 2×2 matrix \hat{G} of the Green functions defined in terms of the initial electron operators. The elements of the matrix \hat{G} are the Green functions \hat{G}_{ij} with $i, j = +, -$ according to whether the time belongs to the upper or the lower branch of the Keldysh contour K . Of these four Green functions only three are independent. Under the operator rotation (6) the Green-Keldysh matrix \hat{G} is transformed as $\hat{G} = \hat{Q}^{-1} \hat{G} \hat{Q}$, where

$$\hat{G} = \begin{pmatrix} \hat{G}^R & \hat{G}^K \\ 0 & \hat{G}^A \end{pmatrix} \quad (8)$$

and

$$\begin{aligned} \hat{G}^R &= i \langle T \psi(t) \psi^\dagger(t^0) \rangle = i \langle T \psi(t) \psi^\dagger(t^0) \rangle; \\ \hat{G}^A &= i \langle T \psi^\dagger(t) \psi(t^0) \rangle = i \langle T \psi^\dagger(t) \psi(t^0) \rangle; \\ \hat{G}^K &= i \langle T \psi(t) \psi(t^0) \rangle = i \langle T \psi(t) \psi(t^0) \rangle; \end{aligned} \quad (9)$$

are respectively retarded, advanced and Keldysh Green functions. Each of these matrices is in turn 2×2 matrix in the Nambu space.

The path integral (5) is now expressed in terms of the new Grassman variables

$$J = \int \mathcal{D}c \mathcal{D}c^\dagger \mathcal{D}\psi \mathcal{D}\psi^\dagger \exp(iS_{\text{dot}} + iS_0[c; c^\dagger]); \quad (10)$$

where

$$S_{\text{dot}} = \int dt c^\dagger \left(i \frac{\partial}{\partial t} - \epsilon_c \right) c + \frac{U}{2} (cc^\dagger)^2; \quad (11)$$

$$\begin{aligned} S_0 &= \int dt \sum_{j=L,R} \int dr_j(r;t) \hat{G}_j^{-1}(r;t) \\ &+ (\Gamma_j(0;t) c(t) + c^\dagger(t) \Gamma_j(t;0)); \end{aligned} \quad (12)$$

Here we defined $\epsilon_c = \epsilon_0 + U/2$. In order to obtain the expression for the operator \hat{G}_j^{-1} we employ the standard Hubbard-Stratonovich transformation of the U^2 -term in (2) and introduce additional path integrals over the complex scalar order parameter field $\psi_j(r;t)$ defined on the Keldysh contour, see e.g. Ref. [15]. Since here we are not interested in the fluctuation effects for the order parameter field, we will evaluate the path integral over ψ_j by means of the saddle point approximation, which amounts to setting $\psi_j(r;t)$ equal to the equilibrium superconducting order parameter values $\psi_{L,R}$ of the left and the right electrodes. If needed, fluctuations of the order parameter field (both the amplitude and the phase) can easily be included into our consideration along the same lines as it was done in Ref. [15]. Disregarding such fluctuations here, we find

$$\hat{G}_{L,R}^{-1}(t) = i \frac{\partial}{\partial t} \psi_L(t) + \psi_L(t) + \psi_R(t); \quad (13)$$

where we define $\psi = (\psi_x - i\psi_y)/2$. Here and below $\psi_x; \psi_y; \psi_z$ is the set of Pauli matrices operating in the Nambu space (for the sake of clarity we chose a different notation from that used for Pauli matrices operating in the Keldysh space).

C. Effective Action

Let us now proceed with the derivation of the effective action for our model. We first notice that the c -fields dependent part S_0 of the total action is quadratic in these fields. Hence, the integrals over c and c^\dagger in (10) can be evaluated exactly, resulting in an action $S_{\text{env}}[c; c^\dagger]$ defined as,

$$\exp(iS_{\text{env}}[c; c^\dagger]) = \int \mathcal{D}\psi \mathcal{D}\psi^\dagger \exp(iS_0[\psi; \psi^\dagger]); \quad (14)$$

Its physical content can be understood as follows; One can say that electrons in two superconducting bulks serve as an effective environment for the quantum dot. Integrating out these electron variables in the spirit of the Feynman-Vernon influence functional approach [16] one arrives at the "environment" contribution to the action S_{env} expressed only in terms of the Anderson impurity variables c and c^\dagger .

Due to the fact that coupling to the leads is concentrated at one point $(x; y) = (0; 0)$ we can integrate out the fields inside the superconductors (hereafter referred as bulk fields) and obtain an effective action in terms of fermion operators with arguments solely on the surface. In order to achieve this central goal let us first note that translation invariance along y permits the Fourier-transform in eq. (12) in this direction. The problem then reduces to a one dimensional one with fermion fields $\psi_k(x)$ where k is the momentum along y . Gaussian integration over the bulk fields can be done with the help of the saddle point method.

$$\hat{G}^{-1}(\mathbf{x}) \tilde{\chi}_k(\mathbf{x}) = 0; \quad (15)$$

Let us decompose $\tilde{\chi}_k(x) = \chi_k^b(x) + \chi_k^s(0)$ in such a way that on the surface one has $\chi_k^b(0) = 0$. The bulk field $\chi_k^b(x)$ satisfies the inhomogeneous equation:

In the right hand side of this equation we employed the standard quasiclassical (Andreev) approximation which makes use of the fact that the superconducting gap as well as other typical energies of the problem are all much smaller than the Fermi energy.

where $v_x = \frac{p_x}{m}$ is the quasiparticle velocity in the x -direction. For a uniform superconducting half-space (here the left one), the Green-Keldysh matrix

(which has the structure (8)) is expressed in terms of the Eilenberger functions [17] as follows:

where

$$\hat{g}^K(\omega) = (\hat{g}^R(\omega) - \hat{g}^A(\omega)) \tanh(\omega/2T): \quad (21)$$

An identical procedure applies for the right electrode. Each superconductor is thus described by a zero-dimensional action, respectively S_L and S_R , coupled by an on-site hopping term with the Anderson impurity. It is now possible to integrate out these surface fields. The integral

can easily be evaluated, so that the contribution of the superconductors to the total effective action of our model is manifested in S_{env} defined as

Note that in deriving (23) we made use of the normalization condition [17] $\mathcal{G}_{\mathrm{L},\mathrm{R}}^2 = 1$.

$$L(R) = 4 \sum_k \frac{T_{L(R)}^2}{V_x}; \quad (24)$$

$$S_{\text{env}} = \frac{i}{2} \int dt \int d^3x \left[\hat{c}^\dagger(t, \mathbf{x}) \left(\hat{L}_L(t; t^0) + \hat{L}_R(t; t^0) \right) \hat{c}(t, \mathbf{x}) \right] \quad (25)$$

The definition (24) requires a comment. Here we consider the situation with one conducting channel in the dot. In this case the transfer amplitudes $T_{L,R}$ should effectively differ from zero only for $j_x = j_y = 0$. One can easily generalize the action (25) to the situation with several or even many conducting channels. In this case the summation over momentum (essentially equivalent to the summation over conducting modes) should be done in (25) and some other dependence of $T_{L,R}^2$ on v_x should apply. For instance, for tunnel junctions in the many channel limit one can demonstrate [18] that $T_{L,R}^2 \propto v_x^3$. It is also quite

clear that the transfer amplitudes $T_{L,R}$ cannot be considered as constants independent of the Fermi velocity direction, as it is sometimes assumed in the literature. In that case the sum (24) would simply diverge at small v_x in a clear contradiction with the fact that quasiparticles with $v_x \neq 0$ should not contribute to the current at all. This "paradox" is resolved in a trivial way: the amplitudes $T_{L,R}$ do depend on v_x and, moreover, they should vanish at $v_x \neq 0$. For further discussion of this point we refer the reader to Ref. [18].

Combining eqs. (10) and (14) we arrive at the expression for the kernel of the evolution operator J solely in terms of the fields c and c^\dagger :

$$J = \int \mathcal{D}c \mathcal{D}c^\dagger \exp(iS_e); \quad S_e[c; c^\dagger] = S_{\text{dot}} + S_{\text{env}}; \quad (26)$$

Here $S_e[c; c^\dagger]$ (defined by eqs. (11) and (25)) represents the effective action for a quantum dot between two superconductors.

D. Transport current

In order to complete our general analysis let us express the current through the dot in terms of the correlation function for the variables c and c^\dagger . This goal can be achieved by various means. For instance, one can treat the superconducting phase difference across the dot as a source field in the effective action and obtain the expression for the current just by varying the corresponding generating functional with respect to this phase difference. Another possible procedure is to directly employ the general expression for the current in terms of the Green-Keldysh functions of one (e.g. the left) superconductor, with arguments at the impurity site:

$$I = \frac{e}{4m} \int dy (\partial_x - \partial_{x^0}) \text{Tr}[G^K(xy; x^0 y^0; t)]_{k=x^0}; \quad (27)$$

where the trace is taken in the Nambu space.

As before, it is convenient to split the bulk and the surface variables. After a simple algebra we transform eq. (27) into the following result:

$$I = \frac{e}{4} \sum_k v_x \text{Tr}[\hat{G}_L \hat{G}^K]_{k,j}; \quad (28)$$

where $G = i \langle c_k(0) c_k^\dagger(0) \rangle$ is the Green-Keldysh function for the surface fields. Here and below the integration over the internal time variables in the product of matrices is implied and $(:::)_k$ means the Keldysh component of this product.

Finally, let us express the function \hat{G} in terms of the correlator for the fields c and c^\dagger . Let us consider the generating functional for the surface fields

$$Z[\eta; \bar{\eta}] = J[T_L z c + \bar{\eta}; T_L z c + \eta]; \quad (29)$$

where the path integral J is defined in (22). The functional derivative of (29) with respect to the fields just yields the function \hat{G} :

$$\hat{G} = i \frac{\delta Z}{\delta \eta} \Big|_{\eta=0}; \quad (30)$$

Evaluating the path integral (29) and making use of (30) we arrive at the following identity

$$i\hat{G} = \frac{2}{v_x} \hat{G}_L z + \frac{4T_L^2}{v_x^2} \hbar c i; \quad (31)$$

Combining (28) and (31) with the condition $\hat{G}_L^2 = 1$ we observe that the contribution of the first term in the right-hand side of (31) to the current vanishes identically, and only the second term $\propto \hbar c i$ turns out to be important. Making use of the definition (24) and symmetrizing the final result with respect to R and L we arrive at the following expression for the current

$$I = \frac{e}{8} \text{Tr}[(\hat{G}_L - \hat{G}_R) \hbar c i]_{j,k} + \hbar c i; \quad (32)$$

This expression completes our derivation. We have demonstrated that in order to calculate the current through an interacting quantum dot between two superconducting electrodes it is sufficient to evaluate the correlator $\hbar c i$ in the model defined by the effective action $S_e = S_{\text{dot}} + S_{\text{env}}$ (11), (25). Our approach enables one to investigate both equilibrium and nonequilibrium electron transport in superconducting quantum dots. In the noninteracting limit $U \rightarrow 0$ the problem reduces to a Gaussian one. In this case it can easily be solved and, as we will demonstrate below, the wellknown results describing normal and superconducting contacts without interaction can be rederived in a straightforward manner. In the interacting case $U \neq 0$ the solution of the problem involves approximations. One of them, the dynamical mean field approximation, is described in the next section.

III. MEAN FIELD APPROXIMATION

In order to proceed further let us decouple the interacting term in (11) by means of a Hubbard-Stratonovich transformation [12,13] introducing additional scalar fields. The kernel J now reads,

$$J = \int \mathcal{D}c \mathcal{D}c^\dagger \mathcal{D}\phi \exp(iS[\phi] + i \int dt c^\dagger \frac{\partial}{\partial t} c - \phi z c); \quad (33)$$

$$S[\phi] = \int dt c^\dagger c + \phi c^\dagger c - \frac{2}{U} \phi^2; \quad (34)$$

These equations are still exact. Now let us assume that the effective Kondo temperature $T_K = U \exp[-j_0 j_2]$ is smaller than the superconducting gap. In this case interactions can be accounted for within the mean field (MF) approximation. The fields in (34) can be determined from the saddle point conditions

$$J = \langle c_x c \rangle = 0; \quad (35)$$

In general these two equations contain an explicit dependence on the time variable. Let us average these equations over time and consider $\langle c_x c \rangle$ as time independent parameters. This approximation is equivalent to retaining only the first moment of $\langle c_x c \rangle$. The self-consistency equations (35) now read

$$\langle c_x c \rangle = \frac{U}{2} \int_{-\infty}^{\infty} dt \langle c_x c \rangle; \quad (36)$$

$$\langle c_x c \rangle = \frac{U}{2} \int_{-\infty}^{\infty} dt \langle c_x c \rangle; \quad (37)$$

As it turns out from our numerical analysis (to be described below), the parameter $\langle c_x c \rangle$ has a negligible effect on the sub-gap current. It just slightly renormalizes the coupling constants $T_{L,R}$ of our model. On the other hand, the second parameter, $\langle c_x c \rangle$, has a large impact on the $I-V$ characteristics. Therefore in what follows we will set $\langle c_x c \rangle = 0$ and take into account only the second self-consistency equation (37) for $\langle c_x c \rangle$. Under this approximation the effective action of our model acquires the following form

$$S_e[\psi] = \int_{-\infty}^{\infty} dt \int_{-\infty}^{\infty} d\epsilon \psi^\dagger(\epsilon) \hat{M}(\epsilon) \psi(\epsilon); \quad (38)$$

$$\hat{M}(\epsilon) = \begin{pmatrix} \epsilon & 0 \\ 0 & \epsilon + i_z (z_L = 2) \hat{g}_L(\epsilon) \end{pmatrix} + i_z (z_L = 2) \hat{g}_L(\epsilon);$$

Here and below we deliberately choose the electrostatic potential of the right electrode to be equal to zero. In this case the Keldysh matrix \hat{g}_R is diagonal in the energy space. Performing the functional integration over Grassmann variables c and c^\dagger we can cast the self-consistency equation (37) for $\langle c_x c \rangle$ in terms of the matrix

$$\hat{M}^{-1} = \begin{pmatrix} \hat{M}^R & 0 \\ 0 & \hat{M}^A \end{pmatrix}^{-1} = \begin{pmatrix} \hat{M}^R & 0 \\ 0 & \hat{M}^A \end{pmatrix}^{-1} \hat{M}^K \begin{pmatrix} \hat{M}^A & 0 \\ 0 & \hat{M}^R \end{pmatrix}^{-1}; \quad (39)$$

where $\hat{M}^R, \hat{M}^A, \hat{M}^K$ are three independent elements of the Keldysh matrix \hat{M} (38). Recall that each of these elements is a 2×2 matrix in the Nambu space and an infinite matrix in the energy space. Eq. (37) for $\langle c_x c \rangle$ can now be rewritten as

$$= i \frac{U}{2} \text{Tr}(\hat{M}^R)^{-1} \hat{M}^K (\hat{M}^A)^{-1}; \quad (40)$$

with the trace being taken both in the energy and spin spaces.

Finally, employing the MF approximation for the Hubbard interaction as was implied in the calculation of $\langle c_x c \rangle$, we get the current as a difference of symmetric forms,

$$I = \frac{e}{8} \text{Tr}[(\hat{N}_L \hat{g}_R^R - (\hat{L} \hat{S} \hat{R})) + \text{h.c.}]; \quad (41)$$

$$\hat{N}_{L,R} = (\hat{M}^R)^{-1} z \hat{g}_{L,R}^K (\hat{M}^A)^{-1};$$

Consider now the case of a constant in time voltage bias V and recall that the entire voltage drop occurs across the quantum dot. Setting the phase of the right electrode equal to zero, for the phase of the left superconductor we obtain $\phi(t) = 2eVt + \phi_0$. Let us express \hat{g}_L in terms of the matrix elements in the energy space [2]

$$\langle \hat{g}_L(\epsilon) \rangle = \sum_{s=0,1}^X (\epsilon^0 + 2seV) \hat{g}_L(\epsilon; +2seV);$$

$$\hat{g}_L(\epsilon; +2seV) = (\hat{g}_L^1(\epsilon - eV)P_+ + \hat{g}_L^{22}(\epsilon + eV)P_-)_{0;s} + e^{i\phi_0} \hat{g}_L^{12}(\epsilon - eV)_{s;1} + e^{-i\phi_0} \hat{g}_L^{21}(\epsilon + eV)_{s;1}; \quad (42)$$

where the superscripts denote the matrix elements in the Nambu space and $P_\pm = (1 \pm z)/2$.

In what follows we shall abbreviate $\hat{g}_L(\epsilon; +2m eV; +2neV) = \langle \hat{g}_L(\epsilon) \rangle_n$ where the right hand side is obtained from eq. (42) after replacing $\phi_0 \rightarrow \phi_0 + 2m eV$, $0;s \rightarrow m;n$, $1;s \rightarrow n;m-1$, and $1;s \rightarrow n;m+1$. Then we have

$$\hat{g}_L(\epsilon;^0) = \sum_n (\epsilon^0 + 2neV) \langle \hat{g}_L(\epsilon) \rangle_n; \quad (43)$$

The matrix \hat{M} (38) may also be represented in a similar form, that is,

$$\hat{M}(\epsilon;^0) = \sum_n (\epsilon^0 + n2eV) \langle \hat{M}(\epsilon) \rangle_n; \quad (44)$$

where

$$\langle \hat{M}(\epsilon) \rangle_n = \begin{pmatrix} \epsilon + m2eV & 0 \\ 0 & \epsilon + n2eV \end{pmatrix} + \frac{i_R}{2} z \hat{g}_R(\epsilon + m2eV)$$

$$+ \frac{i_L}{2} z \hat{g}_L(\epsilon); \quad (45)$$

The integration over energy variables in the self-consistent equation for $\langle c_x c \rangle$ and in the expression for the time averaged current is conveniently performed by dividing the whole energy domain into slices of width $2eV$ and performing energy integration on an interval $[0 < E < 2eV]$. Thus we can use the discrete representation (45) and write

$$= i \frac{U}{2} \sum_{n=0}^X \int_0^{2eV} d\epsilon \text{Tr}(n \hat{M}^R)^{-1} \hat{M}^K (\hat{M}^A)^{-1} \rangle_n;$$

$$I = \frac{e}{8} \text{Tr}[(\hat{N}_L \hat{g}_R^R - (\hat{L} \hat{S} \hat{R})) + \text{h.c.}]; \quad (46)$$

Let us also note that in the case of SAN junctions the expressions for the current and for G can be simplified further. E.g. it is easy to observe that in this case eq. (41) takes the form

$$I = \frac{e}{2} \frac{L}{R} \frac{1}{2} \frac{d}{dz} \text{Tr}[(\hat{M}^R(z))^{-1} \hat{f}(z; V) \hat{M}^A(z)^{-1} \hat{G}_R^R(z) \hat{M}^R(z)^{-1} \hat{f}(z; 0) \hat{G}_R^R(z) \hat{M}^A(z)^{-1} z] + \text{h.c.}; \quad (47)$$

where the matrix \hat{f} has the standard form

$$\hat{f}(z; V) = \begin{pmatrix} \tanh \frac{+eV}{2T} & 0 \\ 0 & \tanh \frac{eV}{2T} \end{pmatrix}; \quad (48)$$

Eq. (47) can be straightforwardly evaluated since the (Fourier transformed) matrices $(\hat{M}^{R,A})^{-1}$ depend now only on one energy (g in (38) is proportional to $(z - 0)$ in this case) and, hence, can easily be inverted analytically. Similar simplifications can also be performed in the self-consistency eq. (40).

IV. RESULTS AND DISCUSSION

A. The SAN junction

1. s-wave superconductors

We start from calculating the differential conductance of an SAN contact assuming the s-wave pairing symmetry in a superconducting electrode. As it was already pointed out above, eqs. (47), (48) allow one to proceed analytically. From these equations one obtains the expression for current which consists of two parts. The first part originates from the integration over sub-gap energies $< \Delta$ and yields the dominating contribution to the current at low temperatures. The other part comes from integration over energies $> \Delta$. At low voltages and temperatures (lower than the gap Δ) this second part gives a negligible contribution to the current. Considering below the sub-gap contribution only, we find

$$I = \frac{e}{4} \frac{L}{R} \frac{1}{2} \frac{d}{dz} B(z) \tanh \frac{+eV}{2T} - \tanh \frac{eV}{2T}; \quad (49)$$

where at sub-gap voltages and energies one has

$$B(z) = \frac{2}{2} \frac{(j_L j_R - j_L j_R)}{2} \frac{L}{R} \frac{1}{\sqrt{2 + \frac{L^2}{4} + \frac{R^2}{4} - \frac{2}{2}}} + \frac{2}{L} \quad (50)$$

and

$$= \frac{1}{2} + \frac{R}{2} \frac{1}{2} \frac{1}{2} : \quad (51)$$

In the limit $eV \ll \Delta$ and $T \rightarrow 0$ for the conductance $G = I/V$ we obtain

$$G = \frac{e^2}{h} \frac{\frac{2}{L} \frac{2}{R}}{\frac{2}{4} + \frac{2}{4} + \frac{2}{2} + \frac{2}{4}} : \quad (52)$$

In order to recover the expression for G in the noninteracting limit in eq. (52) one should simply put $\Delta = 0$. In a symmetric case $L = R$ and for $\Delta \rightarrow 0$ eq. (52) reduces to the well known result [19]

$$G_{NS} = 2G_{NN} = \frac{4e^2}{h}; \quad (53)$$

In the presence of Coulomb interaction the parameter Δ in (50-52) should be determined from the self-consistency equation (40). This equation has a solution provided the interaction U is not very large, i.e. outside the Kondo regime. In the limit of large U the solution of eq. (40) is absent, which indicates the failure of the MF approximation in the Kondo regime.

Here eq. (40) was solved numerically for a given set of the system parameters. In our numerical analysis we chose $L = R = 0.35$ and considered the most interesting sub-gap voltage bias regime $eV < 2\Delta$ in the low temperature limit $T \rightarrow 0$. The values of the Hubbard repulsion parameter U were fixed to be $U = 2.45$ and $U = 2.72$. For convenience we scaled our equations expressing the parameters Δ , U , L, R and T in units of Δ . After that the current and the conductance are normalized respectively in units of e/h and $e^2/2h$.

For the above parameters the value Δ was found to be $\Delta \approx 1.2$ with variations (depending on the voltage) within 10–15 per cents. Thus within a reasonable accuracy in eqs. (50-52) one can consider Δ as constant. On the other hand, even though the variations of Δ with voltage are not large in magnitude, sometimes they occur over a small voltage interval. Therefore such variations may have a considerable impact on the differential conductance $G = dI/dV$ and should also be taken into account. This was done within our numerical analysis. The corresponding results are presented in figure 1.

We observe that for given parameters the conductance virtually vanishes in the substantial part of the sub-gap region. Note, however, that at voltages close to but still smaller than Δ the differential conductance increases sharply. This feature can easily be understood as a result of interplay between Coulomb blockade and two electron tunneling effects. It is well known [19] that the sub-gap conductance in SN junctions is caused by the mechanism of Andreev reflection during which the charge $2e$ is transferred between the electrodes. Without interaction eq. (53) holds down to $V \rightarrow 0$ while in the presence of interaction and at $T = 0$ two electron tunneling process

is completely blocked for $eV < 2E_C$ (see e.g. [20,22]), where $E_C = e^2/2C$ and C is the characteristic junction capacitance. For larger voltages $eV > 2E_C$ two electron tunneling can anymore be blocked by Coulomb effects and the current can flow through the system. Obviously, for $2E_C < \dots$ this results in a finite sub-gap conductance at voltages $2E_C < eV < \dots$. A similar behavior is obtained here (see figure 1) with an important difference, however, that within our model the characteristic Coulomb energy E_C is obtained self-consistently and, hence, it depends not only on the interaction parameter U but also on the voltage V as well as on \dots and \dots . In the case of metallic SIN tunnel junctions the effect of Coulomb interaction on the $I-V$ curve was studied in details both theoretically [22] and experimentally [23].

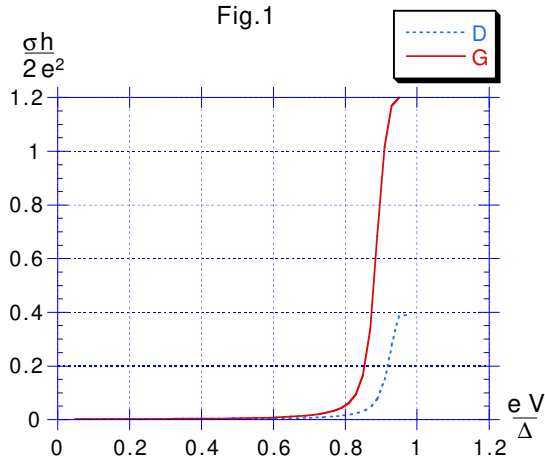


FIG. 1. Differential conductance of an SAN junction with s-wave symmetry superconductor. The figure displays the dependence of Andreev conductance on the applied voltage (in units of superconducting pair potential) for $U = 2.450$ (solid line curve G) and $U = 2.713$ (dotted line curve D). The barrier transparency is $\dots = 0.35$ and the dot level energy is $\dots = 1.5$.

A similar study of an interplay between two-electron tunneling and Coulomb effects in SIS junctions was carried out in Ref. [24].

There exists also a certain analogy between our results and those obtained for superconductor-ferromagnet (SF) junctions [25]. Here the repulsion parameter U plays a role similar to that of an exchange term in SF systems: in both cases the sub-gap conductance can be tuned by changing this parameter in a way that a smaller value of U corresponds to a weaker exchange field. In contrast to our system, however, changing of the exchange field in SF junctions leads to smooth variations of the sub-gap conductance [25].

Let us also note that here we do not consider the Kondo limit [26,28], in which case a zero bias conductance peak is expected. This peak appears, simply, because in the Kondo limit and at $V = 0$ there exists an open channel between the normal metal and the superconductor. Here the Kondo temperature T_K is assumed to be small and, hence, the zero bias peak is absent.

Let us now briefly consider the limit of large bias voltages $eV \dots$. In this case the current may be represented as a sum of two terms $I = I_1 + I_2$. The term I_1 is determined by the expression similar to (49) which now includes the contribution from energies above the gap. We find

$$I_1 = \frac{e}{4} \frac{L_R}{L+R} \frac{1}{2} \frac{d}{dV} [B(\dots) + B_1(\dots)] \tanh\left(\frac{eV}{2T}\right) \quad (54)$$

Here $B(\dots)$ is again given by eq. (50) while the function $B_1(\dots)$ reads

$$B_1(\dots) = \frac{2j_L j_R (j_L^2 + j_R^2)}{[2^2 + (\dots)^2 + 1]} \quad (55)$$

Here we also need

$$1 = \frac{1}{4} \left(\frac{L^2}{L+R} + \frac{R^2}{L+R} + 2 \frac{L_R}{L+R} \right) \quad (56)$$

The other contribution I_2 is proportional to the level position \dots . One obtains

$$I_2 = \frac{e}{4} \frac{L_R}{L+R} \frac{1}{2} \frac{d}{dV} [B_2(\dots) \tanh\left(\frac{eV}{2T}\right) + \dots] \quad (57)$$

The expression for $B_2(\dots)$ can be obtained from eq. (55) if one replaces the term in the square brackets by the expression $2^2(\dots)$.

The above results together with the self-consistency equation for \dots provide a complete description for the $I-V$ curve of an SAN junction in the presence of interactions. In all interesting limits the energy integrals in (54), (57) can be carried out and the corresponding expressions for the current can be obtained. These general expressions, however, turn out to be quite complicated and will not be analyzed in details further below.

Here we just demonstrate that in the noninteracting limit $\dots = 0$ our results reduce to the results already well known in the literature. In the leading order approximation eqs. (54), (55) yield the standard Breit-Wigner formula

$$G = \frac{2e^2}{h} \frac{L_R}{(L+R)^2 + 4} \quad (58)$$

After setting $\tilde{\mu} = 0$ and $\mu_L = \mu_R$ in eqs. (54), (50), (55) in the limit $eV \rightarrow 0$ one easily obtains the contributions to the current equal to $2G_{NN} \mu$ and $G_{NN} (V \pm 2 = 3e)$ respectively from the sub-gap energies (B) and from energies above the gap (B_1). The sum of these contributions yields the standard result

$$I = G_{NN} (V + 4 = 3e): \quad (59)$$

The second term represents the so-called excess current which originates from the mechanism of Andreev reflection. It follows from our general analysis that in quantum dots this current is also affected by Coulomb interaction.

2. Superconductors with unconventional pairing

Since the order parameter for p- and d-wave superconductors is not isotropic, the magnitude of the current is sensitive to the junction geometry. As discussed before, here we consider the system of two planar superconducting (or normal) strips with electron tunneling between them along the x axis through the dot located at $x = y = 0$. For d-wave superconductors we choose the nodal line of the pair potential on the Fermi surface to coincide with the tunneling direction (figure 2), such that $\Delta = v_F p_F \sin 2\theta$.

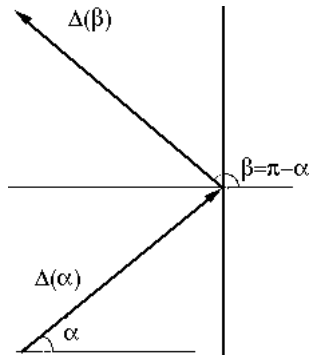


FIG. 2. Schematic geometry of the junction. Incoming and reflected electron-like excitations are moving in an angle-dependent pair potential which can have different signs for these quasiparticles.

The direction of tunneling corresponds to the angle $\theta = 0$. For spin-triplet superconducting states the order parameter is an odd vector function of momentum and a 2×2 matrix in spin space. We choose to represent it by a time reversal symmetry breaking state [9] which is off-diagonal in spin indices. In the geometry of figure 2, θ is the azimuthal angle in the $x-y$ plane and the order parameter can approximately be represented as $\Delta = \Delta_0 \exp(i\theta)$. This order parameter can possibly describe pairing in a superconductor Sr_2RuO_4 which was recently discovered [8]. The pair potential so chosen within the geometry of the junction may have different signs for incoming and reflected quasiparticles moving at the angles θ and $\pi - \theta$, respectively. This fact significantly affects the scattering process and causes the formation of a zero energy (mid-gap) bound state [11] centered at the boundary. For this state we calculate the Green function \hat{G} which, like in the case of s-superconductors, satisfies eq. (16) with a δ -function on the right side and require \hat{G} to vanish at $x = 0$. The distinction of solutions for d- or p-wave superconductors from those found above for the s-wave case is due to the sign change of the pair potential: reflected quasiparticles propagate in a pair potential of an opposite sign as compared to "seen" by incoming quasiparticles. The equilibrium retarded and advanced Eilenberger functions $\hat{G}^{R,A}$ for p-wave superconductors read

$$\hat{G}^{R,A}(\theta) = \frac{p \frac{\Delta}{(i0^+)^2} + \dots}{i0} : \quad (60)$$

The $I-V$ curves for SAN junctions in the case of p-wave superconductors are remarkably distinct from those found for the s-wave case (cf. Figs. 1 and 3). This difference is predominantly due to the surface bound state which exists in the p-wave case and causes the conductance peak in the sub-gap region. Due to electron-electron repulsion this peak is split and appears at $V \neq 0$, see figure 3.

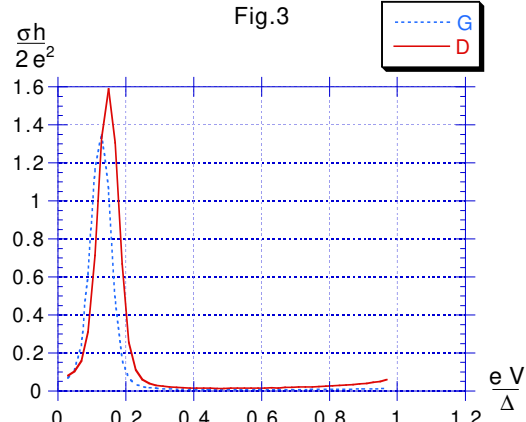


FIG. 3. Same as in figure 1 but for a p-wave symmetry superconductor. The parameters U , μ , and Δ_0 are identical to those of figure 1.

Here again, the repulsion attenuates the conductance, which is larger for $U = 2.45$ than for $U = 2.72$.

B. The SAS junction

Let us start from a noninteracting case $U = 0$ and briefly consider pure resonant tunneling at the Fermi level, i.e. set $\epsilon_0 = 0$. This situation corresponds to a ballistic SNS junction with only one conducting channel. The $I-V$ curves of ballistic SNS junctions were intensively studied in the past [2,29-36]. If the relevant energies are small as compared to Δ (for short junctions this condition usually means $\Delta > \epsilon$), S_{dot} in (26) can be dropped and one gets $\text{hoci} = \hat{g}_+^{-1} z =$. Eq. (32) then yields,

$$I = \frac{e}{2} \text{Tr}_z \hat{g}_+^{-1} \hat{k} : \quad (61)$$

Note that here the tunneling rate just cancels out. In the $\epsilon \rightarrow 0$ limit eq. (61) coincides with the quasi-classical result [29,30]. For a constant bias V the matrix \hat{g}_+^{-1} can be evaluated analytically [31], yielding the $I-V$ curve of a ballistic SNS junction. In particular, in the zero bias limit $V \rightarrow 0$ and for $\Delta \gg \epsilon$ one recovers the MAR current [31]:

$$I_{\text{MAR}} = \frac{2e^2}{h} \frac{2}{eV} V = \frac{4e}{h} : \quad (62)$$

The corresponding explicit calculation performed within our formalism is presented in Appendix. We also note that in the limit of small tunneling rates $\Gamma_{L,R} < \text{resonant}$ effects gain importance. An interplay between MAR and resonant tunneling in the absence of Coulomb interaction was studied in Refs. [35,36].

Let us now turn to SAS junctions with interactions.

1. s-wave superconductors

In order to calculate the sub-gap current in the case of an SAS junction one has first to find the solution of the self-consistency equations (46). This requires the inversion of the matrix \hat{M} in the energy and spin spaces. If the number of modes for each energy in the interval $[0; 2eV]$ is cut off at some integer m , the size of the pertinent matrices is $(4m+2) \times (4m+2)$. The number m of the energy slices has to be adjusted in such a way that the results become insensitive to it. This requires larger m for smaller voltages because quasiparticles can escape the gap region after undergoing a large number of Andreev reflections.

The $I-V$ characteristics for tunneling between two s-wave superconductors is displayed in figure 4.

Fig.4

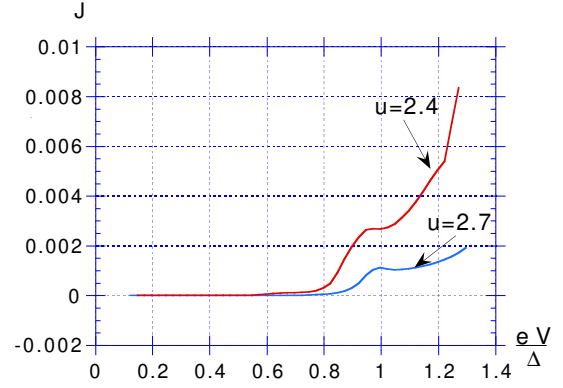


FIG. 4. The subgap tunneling current versus voltage for an SAS junction for which the superconductors pair potential has an s-wave symmetry. The parameters are $U = 2.4; 2.7$, $\Gamma = 1.5$ and $\Delta = 0.6$.

The transparency of the junction is chosen to be $\Gamma = 0.6$ and the current is evaluated for $U = 2.4$ and $U = 2.7$. One observes that at relatively low bias voltages $eV < 0.8$ for $U = 2.4$ and $eV < (0.9; 0.95)$ for $U = 2.7$ the sub-gap current is essentially suppressed. For higher voltages the sub-gap current increases rather sharply, as a result of an interplay between Coulomb blockade and multiple Andreev reflections. The latter mechanism manifests itself in the occurrence of the subharmonic peaks in the differential conductance. Due to interaction, the positions of these peaks are shifted relative to those in the noninteracting case $eV = 2\pi n$, where n is the number of Andreev reflections. As can be seen in figure 4, increasing U results in a larger shift of peak positions.

The behavior observed in figure 4 has a transparent physical interpretation which can be summarized as follows. It is well known that in the absence of interactions the sub-gap conductance of superconducting junctions is determined by the process of multiple Andreev reflections (MAR) with the effective number of such reflections $n \approx 2eV/\Delta$. For the process with given n the charge $(n+1)e$ is transferred between the electrodes. The relevant number n is obviously large at small voltages $eV \ll \Delta$. Let us now turn on the interaction which strength is again characterized by some effective charging energy $E_C = e^2/2C$. Clearly, in this case MAR cycles with large n will be suppressed due to Coulomb effects much stronger than, say, one electron processes simply because in the case $n \gg 1$ the charge much larger than e is being transferred. E.g. at $T = 0$ the single electron processes are blocked for $eV < E_C$, while MAR will be fully suppressed already at higher voltages $eV < (n+1)E_C$. This implies that for relatively small voltages the sub-gap conductance can be effectively suppressed even if the Coulomb energy E_C is small as compared to Δ . This is exactly what we observe in figure

4.

Let us now recall that the sub-harmonic peaks on the $I-V$ curve occur at the voltage values for which quasiparticles participating in MAR cycle with n reflections start leaving the pair potential well. In the presence of interactions this becomes possible if the energy eV_n gained by a quasiparticle (hole) after n reflections is equal to $2 + (n+1)E_C$. This condition immediately fixes the sub-harmonic peak positions at

$$V_n = \frac{E_C}{e} + \frac{2 + E_C}{en}; \quad (63)$$

i.e. due to interaction the sub-harmonic peaks are shifted by $e(1+1/n)=2C$ to larger voltages as compared to the noninteracting case. This feature is fully reproduced within our numerical analysis (see figure 4), which also allows to self-consistently determine E_C as a function of the parameters U , γ , V and ϕ_0 .

Combining the Coulomb blockade condition $eV(n+1)E_C$ with the effective number of Andreev reflections at a given voltage

$$n = \frac{2 + E_C}{eV - E_C}$$

(here $eV > E_C$, in the opposite case no MAR is possible) one easily arrives at the condition

$$eV - E_C = E_C \left(1 + \frac{2}{E_C} \right)^{\#} : \quad (64)$$

This condition determines the voltage interval within which the sub-gap conductance is suppressed due to the Coulomb effects. In the limit $E_C \rightarrow 0$ the corresponding voltage threshold is $eV_{th} = 2E_C$. Finally, by setting $eV_{th} = 2$ into eq. (64) one immediately finds that for

$$E_C = \frac{2}{3}$$

the sub-gap conductance is totally suppressed due to Coulomb interaction and no sub-gap current can flow through the system.

With the aid of eq. (64) we can (roughly) estimate the effective value of E_C for the parameters used in our numerical calculations. From the $I-V$ curves presented in figure 4 we find $E_C \approx 0.2$ for $U = 2.4$ and $E_C \approx 0.25$ for $U = 2.7$. Obviously, these values are smaller than $2/3$ and, hence, the sub-gap conductance is not totally suppressed at intermediate voltages. Substituting the above values of E_C into eq. (63) we can also estimate the magnitudes of the peak shifts with respect to their "noninteracting" values. For $U = 2.4$ the peaks are shifted by 0.3 for $n = 2$ and 0.26 for $n = 3$. Analogous values for $U = 2.7$ are respectively 0.38 and 0.33 . These values are in a reasonably good agreement with our numerical results.

In the limit of high voltages $eV \gg \Delta$ the $I-V$ curves for SAS junctions are analogous to those for SAN ones except the excess current is two times larger.

2. Superconductors with unconventional pairing

Similarly to the case of SAN junctions, there exists an important difference in the tunneling current between SAS junctions depending on whether the order parameter in the electrodes is of s- or p-wave symmetry. The $I-V$ curve for the latter case is depicted in figure 5.

Fig.5

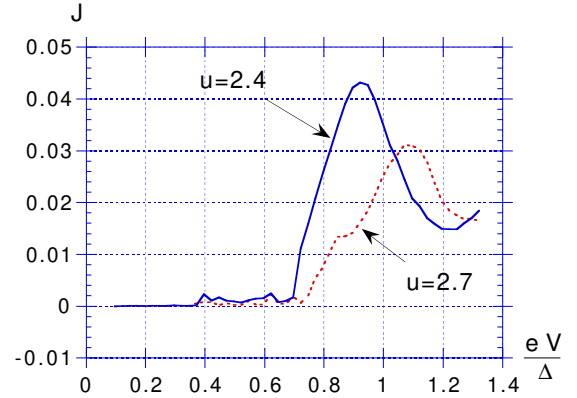


FIG. 5. Same as figure 4 but for superconductors pair potential with p-wave symmetry. The parameters are $U = 2.4$ (dotted curve), $U = 2.7$ (solid curve), $\gamma = 1.5$ and $\phi_0 = 0.6$.

We observe that the sub-gap current for p-wave superconductors is considerably larger than for s-wave ones, roughly by $I_{max}^{(p)} = I_{max}^{(s)} \approx 8$. On the other hand, the effect of the Coulomb repulsion U is rather similar. For $U = 2.7$ the current is suppressed compared to its value at $U = 2.4$. Beside the distinction of magnitudes, there is a novel additional structure in the $I-V$ curves for p-wave superconductors which is related to the presence of a surface bound state. Comparing the results presented in Figs. 4 and 5 we observe that in the latter case, the current peaks at a certain bias voltage. This implies a negative differential conductance, which is the hallmark of resonant tunneling (contributed by the bound state).

Our analysis of the junctions formed by p-wave superconductors can be straightforwardly extended to the case of d-wave pairing. The $I-V$ curves and the sub-harmonic gap structure in junctions with d-wave superconductors in the absence of Coulomb interaction was recently studied (see e.g. Ref. [37] and other Refs. therein). Near zero bias the $I-V$ curves [37] exhibit a current peak (equivalently, negative differential conductance) related to the presence of the mid-gap surface states. Notice, that in such systems the symmetry restricts the current, so that the contribution from the bound mid-gap states may van-

ish if, for instance, one assumes $T_{L,R}^2$ to be independent of v_x . As we have already argued before (see also Ref. [18]), it might be essential to take the dependence of tunneling matrix elements on v_x into account already for point contacts. One can also consider the impurity model different from a point-like defect. Such a situation can be realized e.g. by artificially-induced defects [38]. The spectroscopy of $Bi_2Sr_2CaCu_2O_8$ surfaces indicates that such defects appear to be more extended in STM imaging. In this case one can expect non-zero contribution from mid-gap level also in d-wave superconductors. Here, again, the electron-electron repulsion shifts the peak positions from their "noninteracting" values $eV = 2\epsilon_n$ to higher voltages. It is quite likely that this interaction-induced shift was observed in the experiment [39].

V. CONCLUSIONS

In this paper the tunneling between two superconductors or between a superconductor and normal metal through an Anderson-type quantum dot is investigated. Special attention is devoted to analyze the implications of the Coulomb repulsion between electrons in the dot on the tunneling process. The Andreev conductance for an SAN junction and the sub-gap current in an SAS junction are calculated and elaborated upon. The theoretical treatment requires a combination of the Keldysh non-equilibrium Green function and path integral formalism and the dynamical mean field approximation. We derive general expressions for the effective action and the transport current through the system. These expressions are then employed in order to obtain a workable formula for the current. The latter is then calculated analytically and numerically for a certain set of energy parameters.

The main results of the present research can be summarized as follows: 1) When one of the electrodes is a normal metal (an SAN junction) the gap symmetry structure is exhibited in the Andreev conductance. For p-wave superconductors, it shows a remarkable peak for voltages in the sub-gap region. For s-wave superconductors, on the other hand, the position of the peak is shifted towards the gap edge. It is further demonstrated that if the Hubbard repulsive interaction increases the current peak at the gap edge is strongly suppressed. 2) The dynamics of tunneling between two superconductors (an SAS junction) is more complicated. For s-wave superconductors the usual peaks in the conductance that originate from multiple Andreev reflections [2] are shifted by interaction to higher values of V . They also suffer sizable suppression as the Hubbard interaction strength increases. The sub-gap current in this case may describe the low energy channels in break junctions [6]. For p-wave superconductors, the sub-gap current is much larger than in the s-wave case and the $I-V$ characteristics exhibits a novel feature: the occurrence of mid-gap bound state results in

a peak in the current, that is, a negative differential conductance.

Acknowledgments: This research is supported in part by grants from the Israeli Science Foundation (Center of Excellence and Non-Linear Tunneling), the German-Israeli DIP foundation Quantum Electronics in Low Dimensional Systems and the US-Israel BSF grant Dynamical Instabilities in Quantum Dots.

V I. APPENDIX

Below we will derive the result (62) within the framework of the formalism developed in the present paper. Consider a quantum dot between two s-wave superconductors and assume that the interaction is negligibly small $U \rightarrow 0$. For the sake of simplicity we will also set $\epsilon_L = \epsilon_R = 0$. The result (41) can be expressed as a sum of two terms $I = I_{AR} + I_{qp}$, where

$$I_{AR} = \frac{e^2 Z}{4h} \int_0^{2eV} d\text{Tr}[\tilde{N}_R^{12} (\mathcal{G}_L^A)^{21} \tilde{N}_L^{12} (\mathcal{G}_R^A)^{21} \tilde{N}_R^{21} (\mathcal{G}_L^R)^{12} + (\tilde{N}_L)^{21} (\mathcal{G}_R^R)^{12}]; \quad (65)$$

$$I_{qp} = \frac{e^2 Z}{4h} \int_0^{2eV} d\text{Tr}[\tilde{N}_R^{11} (\mathcal{G}_L^A \mathcal{G}_L^R)^{11} \tilde{N}_L^{11} (\mathcal{G}_R^A \mathcal{G}_R^R)^{11}]; \quad (66)$$

Here I_{AR} is the sub-gap (Andreev reflection) contribution to the averaged current while I_{qp} is defined by the excitations above the gap. In (A.1)-(A.2) we defined the Green-Keldysh matrices $\mathcal{G} = i_z \hat{g}$ with

$$\mathcal{G}_{R,L}^{R,A}(\epsilon) = F^{R,A}(\epsilon) \left(\frac{1}{\epsilon - \epsilon_F} + \frac{1}{\epsilon - \epsilon_F + i0} \right); \quad (67)$$

$$F^{R,A}(\epsilon) = \frac{1}{2} \frac{(j_j - j_j)}{2} \text{sign} \left(\frac{(j_j - j_j)}{2} \right); \quad (68)$$

$$\mathcal{G}_{R,L}^K(\epsilon) = (\mathcal{G}_{R,L}^R(\epsilon) - \mathcal{G}_{R,L}^A(\epsilon)) \tanh(\epsilon/2T); \quad (69)$$

We also defined

$$\tilde{N}_{L,R}^{ij} = (\tilde{M}^R \mathcal{G}_{L,R}^K \tilde{M}^A)^{ij}; \quad \tilde{M}^{R,A} = (\tilde{M}^{R,A})^{-1}; \quad (70)$$

where the superscripts stand for the spin indices in Nambu space and Tr denotes the remaining trace over (discrete) energies which are scaled to throughout this Appendix.

Consider the limit of small voltages $eV \rightarrow 0$. In this limit the sub-gap current I_{AR} can be rewritten in the form

$$I_{AR} = \frac{e^2 V}{h} \sum_{m,n} \mathcal{G}^K(E_m) ((m | \tilde{M}^A)^{i2} | n) (n + 1 | \tilde{M}^R)^{1i} | n) F^A(E_n^+) (m | \tilde{M}^A)^{i1} | n) (n - 1 | \tilde{M}^R)^{2i} | n) F^R(E_n^-)$$

$$\begin{aligned}
& g^K(E_m) ((m j M^A)^{12} j_n) \\
& (n j M^R)^{11} j_n F^A(E_n) - (m j M^A)^{11} j_n \\
& (n j M^R)^{21} j_n F^R(E_n)) \\
& g^K(E_m^+) ((m j M^A)^{22} j_n) \\
& (n j M^R)^{12} j_n F^A(E_n) - (m j M^A)^{21} j_n \\
& (n j M^R)^{22} j_n F^R(E_n))]: \quad (71)
\end{aligned}$$

Here we denote $E_n = eV(2n+1)$ and $E_n = 2eVn$. We also included $n=2$ into the definition of M^R and omitted terms non-diagonal in the spin indices because these terms are small in the limit $eV \rightarrow 0$. At $T \rightarrow 0$ the summation over m is reduced to just one term with the maximum number m_0 determined by the condition: $j_{m_0} = 1$.

It is straightforward to evaluate the matrices $(m_0 j M^{ij} j_n)$ for sufficiently large n and $m_0 \rightarrow 0$. In this case M^{ij} satisfy the following approximate equations

$$\begin{aligned}
& (m j M^R)^{11} j_{n_0} (E_m^2 = 4 - 2) = \\
& E_{m-m_0} = 2F^R(E_m) \\
& + (m-1 j M^R)^{11} j_{n_0} + (m+1 j M^R)^{11} j_{n_0}); \quad (72)
\end{aligned}$$

$$\begin{aligned}
& (m j M^R)^{12} j_{n_0} = -4 (m j M^R)^{12} j_{n_0} \\
& (E_m F^R(E_m) E_{m_0} F^R(E_{m_0})^{-1}); \quad (73)
\end{aligned}$$

$$\begin{aligned}
& (m j M^R)^{12} j_{n_0} (E_m^2 = 4 - 2) = \\
& [m-m_0 + m-1-m_0] E_m^2 F^R(E_m) = 4 \\
& + (m-1 j M^R)^{12} j_{n_0} + (m+1 j M^R)^{12} j_{n_0} \quad (74)
\end{aligned}$$

Similar equations can easily be derived for the two remaining blocks. In the leading order in m_0 (this approximation is justified at small voltages $V \rightarrow 0$) at sub-gap energies ($E_n < 1$, $F^R = F^A = F$) we obtain

$$(n j M^R)^{11} j_{n_0} = \frac{(1)^n (n+1)}{(m_0+2)F(E_{m_0})}; \quad (75)$$

$$(n j M^R)^{12} j_{n_0} = \frac{(1)^n (n+1)E_{m_0}}{(m_0+2)E_n F(E_n)}; \quad (76)$$

$$(n j M^R)^{21} j_{n_0} = \frac{(1)^n (n+1)E_{m_0}}{(m_0+2)E_n F(E_n)}; \quad (77)$$

Substituting these matrix elements into eq. (A.7) and performing a simple summation over n we arrive at the result (62).

email: yshai@bgumailbgu.ac.il

- [1] T.M. Klapwijk, G.E. Blonder, and M. Tinkham, Physica 109+110B, 1157 (1982).
[2] G.B. Arnold, J. Low Temp. Phys. 59, 143 (1985).

- [3] A. Golub, Phys. Rev. B 54, 1526 (1995).
[4] L.I. Glazman and K.A. Matushev, Zh. Eksp. Teor. Fiz. Pis'ma Red. 49, 570 (1989) [JETP Lett. 49, 659 (1989)].
[5] D.C. Ralph, C.T. Black, and M. Tinkham, Phys. Rev. Lett. 74, 3241 (1995).
[6] E. Scheer et al., Phys. Rev. Lett. 79, 3535 (1997); J.M. van Ruitenbeek, cond-mat/9910394.
[7] J.C. Cuevas, A. Levy Yeyati, and A. Martin-Rodero, Phys. Rev. Lett. 80, 1066 (1998).
[8] Y. Maeno et al., Nature 372, 532 (1994).
[9] T.M. Rice and M. Sigrist, J. Phys. Condens. Matter 7, 643 (1995).
[10] L. Buchholtz and G. Zwicknagl, Phys. Rev. B 23, 5788 (1981).
[11] C.-R. Hu, Phys. Rev. Lett., 72, 1526 (1994).
[12] A.V. Rozhkov and D.P. Arovas, Phys. Rev. Lett. 82, 2788 (1999).
[13] Y. Avishai and A. Golub, Phys. Rev. B 61, 11293 (2000).
[14] L.V. Keldysh, Zh. Eksp. Teor. Fiz. 47, 1515 (1964) [Sov. Phys. JETP 20, 1018 (1965)].
[15] G. Schon and A.D. Zaikin, Phys. Rept. 198, 237 (1990).
[16] R.P. Feynman and F.L. Vernon Jr., Ann. Phys. (NY) 24, 118 (1963); R.P. Feynman and A.R. Hibbs, Quantum Mechanics and Path Integrals (McGraw Hill, NY, 1965).
[17] G. Eilenberger, Z. Phys. 214, 195 (1968); A.I. Larkin and Yu.N. Ovchinnikov, Zh. Eksp. Teor. Phys. 68, 1915 (1975) [Sov. Phys. JETP 41, 960 (1975)]. For a recent review see also W. Belzig, F.K. Wilhelm, C. Bruder, G. Schon and A.D. Zaikin, Superlattices and Microstructures 25, 1251 (1999).
[18] Yu.S. Barash, A.V. Galaktionov, and A.D. Zaikin, Phys. Rev. B 52, 665 (1995); Phys. Rev. Lett. 75, 1675 (1995).
[19] G.E. Blonder, M. Tinkham, and T.M. Klapwijk, Phys. Rev. B 25, 4515 (1982).
[20] F.W. J. Hekking et al., Phys. Rev. Lett. 70, 4138 (1993).
[21] F.W. J. Hekking and Yu.V. Nazarov, Phys. Rev. Lett. 71, 1625 (1993); Phys. Rev. B 49, 6847 (1994).
[22] A.D. Zaikin, Physica B 203, 255 (1994).
[23] J.M. Hergenrother, M. Tuominen, and M. Tinkham, Phys. Rev. Lett., 72, 1742 (1994).
[24] J. Siewert, Europhys. Lett. 46, 768 (1999).
[25] M.J.M. de Jong and C.W.J. Beenakker, Phys. Rev. Lett., 74, 1657 (1995).
[26] A. Golub, Phys. Rev. B 54, 3640 (1996).
[27] R. Fazio and R. Raimondi, Phys. Rev. Lett. 80, 2913 (1998).
[28] A.A. Clerk, V. Ambegaokar, and S. Hershfield, cond-mat/9901205.
[29] A.V. Zaitsev, Zh. Eksp. Teor. Fiz. 78, 221 (1980) [Sov. Phys. JETP 51, 111 (1980)].
[30] A.D. Zaikin, Zh. Eksp. Teor. Fiz. 84, 1560 (1983) [Sov. Phys. JETP 57, 910 (1983)].
[31] U. Günsenheim and A.D. Zaikin, Phys. Rev. B 50, 6317 (1994).
[32] D.V. Averin and D. Bardas, Phys. Rev. Lett. 75, 1831 (1995).
[33] E.N. Bratus, V.S. Shumeiko, and G. Wendin, Phys. Rev. Lett. 74, 2110 (1995).
[34] J.C. Cuevas, A. Martin-Rodero, and A. Levy Yeyati, Phys. Rev. B 54, 7366 (1996).

- [35] A . Levy Yeyati, J.C . Cuevas, A . Lopez-D avalos, and A .
M artin-R otero, Phys. Rev. B 55, R 6137 (1997).
- [36] G . Johansson, E.N . Bratus, V.S. Shum eiko, and G .
W endin, Phys. Rev. B 60, 1382 (1999).
- [37] T . Lofwander, G . Johansson, and G . W endin, cond-
m at/9908261.
- [38] A . Yazdani et al, Phys. Rev. Lett. 83, 176 (1999).
- [39] A . Engelhardt, R . D ittm ann, and A .I. Braginski, Phys.
Rev. B 59, 3815 (1999).